



OPEN ACCESS

EDITED BY

Yogan Khatri, Cayman Chemical, Ann Arbor, United States

Su Sun.

Wuchang Shouyi University, China

Marcin Sajdak,

Silesian University of Technology, Poland

*CORRESPONDENCE

Wolfgang R. Streit, \bowtie wolfgang.streit@uni-hamburg.de

RECEIVED 21 July 2025 ACCEPTED 29 September 2025 PUBLISHED 31 October 2025

Wongwattanarat S, Schorn A, Klose L, Carré C, Malvis Romero A. Liese A. Pérez-García P and Streit WR (2025) A combined chemo-enzymatic treatment for the oxidation of epoxy-based carbon fiber-reinforced polymers (CFRPs). Front. Bioeng. Biotechnol. 13:1670548. doi: 10.3389/fbioe.2025.1670548

COPYRIGHT

© 2025 Wongwattanarat, Schorn, Klose, Carré, Malvis Romero, Liese, Pérez-García and Streit. This is an open-access article distributed under the terms of the Creative Commons Attribution License (CC BY). The use, distribution or reproduction in other forums is permitted, provided the original author(s) and the copyright owner(s) are credited and that the original publication in this journal is cited, in accordance with accepted academic practice. No use, distribution or reproduction is permitted which does not comply with these

A combined chemo-enzymatic treatment for the oxidation of epoxy-based carbon fiber-reinforced polymers (CFRPs)

Sasipa Wongwattanarat¹, Andrea Schorn¹, Leon Klose², Camille Carré³, Ana Malvis Romero², Andreas Liese², Pablo Pérez-García¹ and Wolfgang R. Streit¹*

¹Department of Microbiology and Biotechnology, University of Hamburg, Hamburg, Germany, ²Institute of Technical Biocatalysis, Hamburg University of Technology, Hamburg, Germany, ³Airbus Defence and Space GmbH, Central Research and Technology, Munich, Germany

Carbon fiber-reinforced polymers (CFRPs), particularly epoxy-based composites, have become essential in the aerospace, automotive, and wind energy industries due to their robust mechanical properties, and lightweight nature. However, there is a lack of recycling technologies that are environmentally sustainable while also ensuring the recovery of carbon fibers in their original state. Although certain bacterial and fungal strains can colonize epoxy polymers, enzymes capable of efficiently degrading these materials have not yet been reported. Consequently, there is an urgent need for an effective, sustainable, and biologically inspired solution for CFRP recycling. Here, a chemo-enzymatic two-step oxidation process was developed. A chemical pre-treatment with propionic acid and hydrogen peroxide was used to recover imbedded carbon fibers. Additionally, three novel bacterial laccases isolated from a European spruce bark beetle gut metagenome (Ips typographus) demonstrated the ability to oxidize three epoxy resin scaffolds derived from TGMDA-based epoxy resin system, a high-performance material commonly used in aerospace applications. The sequential combination of both oxidative steps enabled the retrieval of clean carbon fibers and showed the potential of the laccase to partially further modify the pre-treated cured epoxy. This bio-inspired approach marks an initial step toward developing a bio-based recycling method for epoxy CFRPs.

KEYWORDS

epoxy resin, CFRP, oxidation, laccase, multicopper oxidase

1 Introduction

Epoxy polymers are thermosetting polymers that are essential in materials engineering due to their exceptional mechanical properties, as well as their high thermal and chemical resistance (Sukanto et al., 2021). These characteristics stem from a strong three-dimensional network formed during the curing process of epoxy resins and hardeners (Jin et al., 2015). Typically containing two or more oxirane groups, epoxy resins can be tailored to specific applications by combining them with various hardeners or curing agents like aliphatic and aromatic amines, anhydrides, thiols, and acids (Karak, 2021). This versatility makes them a

preferred choice for carbon fiber-reinforced polymers (CFRPs) in industries such as aerospace, automotive, and construction, where lightweight, strength, and durability are crucial (Aamir et al., 2019; Ahmad et al., 2020). Notably, CFRPs constitute up to 53% by weight of current commercial aircraft structures (Gondaliya et al., 2016). Global demand for CFRPs is increasing by approximately 10% annually (Schüppel, 2023), with projected global production expected to reach 285,000 tons by 2025 (Zhang S. et al., 2023). Additionally, an estimated 7,000 aircraft are expected to be retired by 2036 (Bombardier, 2017; Scheelhaase et al., 2022), and the aircraft industry alone is projected to generate approximately 500,000 tons of CFRP waste annually by 2050 (Meng et al., 2020). These trends indicate significant volumes of CFRP waste are likely to enter the waste stream in the coming decades, raising concerns over the need for effective disposal and recycling strategies.

Various recycling methods have been explored, with chemical recycling, or solvolysis, holding most promising for recovering both carbon fibers and matrix polymers (Liu et al., 2022). However, challenges remain in identifying solvents with low environmental impact that can operate under low temperature and pressure (Cheng et al., 2017). Despite progress, there is still a lack of sustainable, biologically inspired approach for degrading epoxy-based CFRPs (eCFRPs) (Klose et al., 2023).

The biodegradation of epoxy polymers remains challenging due to their synthetic nature: extensive cross-linking, stable chemical motifs (i.e., ethers and tertiary amines), and a lack of easily hydrolysable linkages. While some bacteria like Pseudomonas sp. and Bacillus flexus can colonize and reduce the corrosion resistance of epoxy coatings (Wang et al., 2016; Deng et al., 2019), significant advancements in identifying microorganisms capable of efficient degradation, similar to Ideonella sakaiensis with polyethylene terephthalate (PET), have yet to be achieved (Yoshida et al., 2016). Several studies have attempted to identify microorganisms with potential to degrade cured epoxy and eCFRPs (Negi et al., 2009; Gu et al., 1997; Pardi-Comensoli et al., 2022), but none provide definitive evidence of substantial degradation at micro- or millimolar levels, and the specific enzymes involved remain unidentified. Among previously identified enzymes, laccases (EC 1.10.3.2), have shown potential in partially and randomly oxidizing the surface of recalcitrant synthetic polymers [e.g., polyethylene (PE), polyvinyl chloride (PVC)] (Temporiti et al., 2022; Zhang et al., 2022), even though they do not significantly degrade the polymer backbone.

Laccases, or multi-copper oxidases (MCOs), can oxidize complex lignin-derived molecules with cross-linked ether and carbon-carbon bonds, as well as phenolic and non-phenolic compounds, by reducing molecular oxygen to water. These versatile enzymes catalyze various oxidative reactions, including phenolic oxidation, aromatic hydroxylation, oxidative polymerization, and demethylation (Munk et al., 2015; Bassanini et al., 2021), making them potential enzymes for modifying complex organic compounds with applications in biotechnology and environmental remediation (Khatami et al., 2022). Moreover, the laccase-mediator system (LMS) has evolved in nature to broaden their substrate range, with mediators (e.g., ABTS (2,2'-azino-bis(3-ethylbenzothiazoline-6-sulfonic acid))) acting as electron shuttles (Hilgers et al., 2018). In contexts where natural enzymatic pathways struggle with recalcitrant synthetic polymers, laccases present a potential solution to the challenges posed by epoxy polymers.

This study developed a chemo-enzymatic treatment for the two-step oxidation of eCFRPs. Alternative pre-treatments were explored, with propionic acid/H₂O₂ at 65 °C and atmospheric pressure effectively decomposing diglycidyl ether of bisphenol A (DGEBA)-based composites while recovering clean carbon fibers with potential for reuse. Three novel bacterial laccases, isolated from the bark beetle (*Ips typographus*), were screened for their potential activity on three structural scaffolds of a tetraglycidyl methylene dianiline (TGMDA)-based epoxy commonly used in aerospace applications. Our findings demonstrate that laccase can convert soluble oligomers generated during the pre-treatment of cured epoxy and further partially modify exposed functional groups on the pre-treated polymer surface, representing an initial step toward developing a bio-based recycling strategy for eCFRPs.

2 Materials and methods

2.1 Bark beetle sample collection

Bark beetle specimens were collected using Theysohn slot traps (Niemeyer et al., 1983) baited with the beetle pheromone Ipsowit (Witasek, Austria) and stored at -20 °C immediately after collection. The beetles were disinfected with 96% ethanol and affixed to paraffin plates with their ventral abdomen facing upward. During dissection, immobilized beetles were submerged in sterile 1X phosphate-buffered saline (PBS) pH 7.4. The intestines were extracted and stored at -20 °C.

2.2 DNA extraction and sequencing

Metagenomic sequencing of Ips typographus DNA was performed at the Heinrich Pette Institute in Hamburg, Germany. A genomic library was prepared using the NEBNext[®] Ultra[™] DNA Library Prep Kit for Illumina® (New England BioLabs, Germany), and quality-checked with a BioAnalyzer High Sensitivity Chip (Agilent Technologies Inc., United States). Sequencing was performed on an Illumina HiSeq 2500 instrument (Illumina Inc., United States) in paired-end mode, generating 2 \times 125 bp reads. Data were processed with Trimmomatic software v.0.32 (Bolger et al., 2014) for quality trimming and assembled using IDBA-UD software v.1.1.1 (Peng et al., 2012). The dataset was uploaded to the GOLD database (Kyrpides, 1999), annotated via the DOE-JGI pipeline (Huntemann et al., 2015), and stored in the IMG database (Markowitz et al., 2012) with gene ID: ItL-01, Ga0063521_ 10002204; ItL-02, Ga0063521_100014138; ItL-03, Ga0063521_ 100024328; ItL-04, Ga0063521_1000001282; ItL-05, Ga0063521_ 100021622; ItL-06, Ga0063521_100028714. A search was performed in the IMG metagenome using the keyword "multicopper oxidase". Six candidate genes, with completeness and the presence of all four conserved copper-binding site (CBS) motifs, are listed in Supplementary Table S1.

2.3 Bioinformatic analysis

Amino acids of the putative and the recognized laccases were acquired from public sequence databases NCBI, UniProt, and IMG

(Author anonymous, 2018; The UniProt Consortium, 2017; Markowitz et al., 2012). Local alignments were performed with BLASTp (Boratyn et al., 2012). The sequence alignment of the amino acid sequences was conducted using the T-Coffee server with Expresso mode (Armougom et al., 2006). The phylogenetic tree was constructed using MEGA11 with maximum-likelihood method and JTT matrix-based model with 1,000 bootstrap replicates (Tamura et al., 2021). The 3D structural models were predicted using AlphaFold 3 (Abramson et al., 2024). The evolutional conservation profiles of the proteins were analyzed using Consuf server (Yariv et al., 2023). The models were visualized using UCFS Chimera v.1.16 (Huang et al., 2014).

2.4 Molecular cloning, protein expression, and purification

The MCO genes were synthesized with codon optimization for E. coli (MWG Eurofins, Germany). The strains, plasmids and primers used are listed in Supplementary Table S2. Genes were inserted into pET21a (+) expression vectors. ItL-01-03 were transformed into E. coli BL21 (DE3) (Novagen/Merck, Germany), while CueO was transformed into E. coli T7 Shuffle (New England BioLabs, Germany). An overnight inoculum (1%) was grown aerobically in autoinduction medium (ZYM-5052; Studier, 2005), with 100 μg/mL ampicillin at 37 °C until an OD₆₀₀ of 0.6 was reached. Cultures were then supplemented with 250 μM CuSO₄ and incubated at 28 °C for 16-20 h. Cells were harvested, treated with 1 mM phenylmethanesulfonyl fluoride (PMSF), and lysed three times at 1,250 psi using a French press (American instrument, United States). Proteins were purified with Ni-NTA agarose (Qiagen, Germany) and dialyzed in 50 mM Tris-HCl pH 7 using a 30 kDa Amicon tube (GE Healthcare, Germany).

2.5 Biochemical characterization

A series of spectrophotometric assays using 2,2'-azino-di-(3-ethylbenzthiazoline sulfonic acid) (ABTS; Merck, Germany) was performed to characterize the recombinant laccases, with a detectable color at 420 nm (ϵ = 36,000 M⁻¹ cm⁻¹), measured using a Synergy HT microplate reader (BioTek, Germany).

In each assay, 2 μ M laccase was incubated with 1 mM ABTS in a total volume of 200 μ L within a 96-well plate, supplemented with 1 mM CuSO₄. Initial tests determined optimal pH using 0.1 M citrate-phosphate buffers from pH 3 to 7, followed by temperature optimization from 20 °C to 80 °C. Buffer preference was evaluated with 0.1 M citrate-phosphate and acetate buffers at their respective optimal pH levels. Thermostability assays were conducted at 30 °C–60 °C for 7 days. The effect of Cu²⁺ supplementation (0 μ M–1 mM) was tested in 0.1 M acetate buffer at pH 4 and optimal temperatures (T_{opt}).

Kinetic constants were determined using ABTS in 200 μ L, 0.1 M acetate buffer pH 4 at 25 °C for 30 min. The Michaelis-Menten constant ($K_{\rm m}$), maximum reaction rate ($V_{\rm max}$), and turnover rate ($K_{\rm cat}$) were calculated by fitting the initial rates to the Michaelis-Menten equation with Solver (Microsoft Excel add-in, Frontline Systems, Inc., United States) (Supplementary Figure S3) (Chris and Nithesh Chandrasekharan, 2020).

Laccase ItL-03 was characterized for optimal pH with substrates ABTS, syringol, guaiacol (Merck, Germany) using 0.1 M buffers: citrate-phosphate (pH 3-6), phosphate (pH 6-8), Tris (pH 8-9), and carbonate-bicarbonate (pH 9-10), with 3 mM substrate and 5 mM CuSO₄. Specific activity (U/mg) was evaluated with 1 mM substrate and 1 mM CuSO₄, monitoring absorbance over 3 min at ϵ 420 = 36,000 M⁻¹ cm⁻¹ for ABTS, ϵ 468 = 14,800 M⁻¹ cm⁻¹ for syringol, and ϵ 465 = 12,000 M⁻¹ cm⁻¹ for guaiacol.

2.6 Assessment of enzymatic activities on epoxy surrogates

The oxidative activity of laccases on bis(4-dimethylaminocyclohexyl) methane (BBCM; kindly donated by the Institute of Technical Biocatalysis, Hamburg University of Technology, Germany), 1,3-bis(methyl (phenyl)amino) propan-2-ol (BMAP; kindly contributed by the Manchester Institute of Biotechnology, University of Manchester, United Kingdom), and N, N-bis(2hydroxypropyl)-p-toluidine (NNBT; Toronto Research Chemicals, Canada) was investigated. These substrates were dissolved in dimethyl sulfoxide (DMSO) to prepare 100 mM stock solutions. In each reaction, 0.02 U/mg of purified enzyme was incubated with 3 mM substrate, 1 mM CuSO₄, and 1 mM ABTS in 0.1 M acetate buffer pH 4 at Topt. The mixture was shaken at 450 rpm for 2 h. For endpoint analysis, samples were diluted 1:3 with buffer, centrifuged at 13,000 rpm for 6 min, then extracted with dichloromethane (DCM) in a 1:1 ratio and centrifuged again. The DCM layer was diluted 100-fold in LC-MS grade water.

2.6.1 Liquid chromatography-mass spectrometry (LC-MS)

LC analysis was performed using a Dionex Ultimate 3000 UHPLC system with an Agilent Zorbax Extend-C18 column (2.1 \times 50 mm, 1.8 μm). The mobile phase was acetonitrile and water with 0.1% (v/v) formic acid, with a gradient from 5% to 95% acetonitrile over 28 min at a flow rate of 0.3 mL/min, monitored at 254 nm. Mass detection used a Bruker maXis ESI-QTOF in positive mode (m/z 50-2300, capillary voltage 4 kV). Data were analyzed using MestReNova x64 (Mestrelab Research S.L.U, Spain). To evaluate the enzymatic activity of ItL-03 on NNBT, LC system was replaced with an Agilent 1260 HPLC, and the run time was extended to 30 min, with other parameters remained unchanged. Analyte concentrations were determined via calibration curves (Supplementary Figure S5). The initial concentration at t_0 was set at 100%, and the conversion rate was calculated by subtracting the remaining epoxy from 100%.

2.7 Pre-treatment analysis of CFRPs

Carbon fiber-epoxy resin (eCFRPs) was purchased from Goodfellow, Ltd., Germany (product code C-42-SH-000150; SKU: 1000037921; 0.5 mm thickness; 150 \times 150 mm). The material comprises Toray T300 carbon fiber (or equivalent) with 50% volume fraction and Elantas EC157 epoxy resin (or equivalent). The detailed information on the epoxy formulation and curing is not provided by the manufacturer. The diglycidyl ether of bisphenol A

(DGEBA)-based composite was laser-cut into 6 \times 12 mm pieces. Samples were incubated in various acidic-peroxide solutions, containing either 5 M or 9 M acid and H_2O_2 in a 95:5 ratio. The solution volume was 60 mL/g, and treatments lasted 8, 24, and 48 h at 65 °C with continuous shaking at 200 rpm. Control samples were exposed to acid, H_2O_2 , and water. After treatment, samples were washed thoroughly with warm water and dried overnight at 60 °C. The mass fraction of resin was determined following DIN EN 2564: 2018 (eVD, 2019). The resin weight loss rate was calculated based on established methods (Das et al., 2018).

2.7.1 Fourier transform infrared (FTIR) spectroscopy

FTIR spectra were recorded using a Vertex 70v spectrometer (Bruker, Germany) in ATR mode. Pre-treatment analysis of CFRPs was analyzed over a spectral range of 4,000 to 650 cm⁻¹, at a resolution of 2 cm⁻¹, with each spectrum generated from 50 scans at 27 °C. The measurements of the TGMDA-based epoxy powder used in chemo-enzymatic treatment were conducted similarly, but over a range of 4,000 to 600 cm⁻¹ with 32 scans. Data were processed using OPUS software (Bruker, United States), normalized to [0, 1], and smoothed with a Savitzky-Golay filter (20 points) using OriginPro 2024 (OriginLab Inc., United States).

2.7.2 Scanning electron microscopy (SEM) analysis

Imaging was performed with a LEO 1525 Field Emission Scanning Electron Microscope (LEO Electron Microscopy Inc., United States), operating at an electron high tension (EHT) of 5–10 kV and a working distance (WD) of 8.1–9.6 mm. Data was processed using SmartSEM V06.00 software (Carl Zeiss Microscopy GmbH, Germany).

2.7.3 Energy-dispersive X-ray (EDX) spectroscopy

Elemental analysis of the carbon fibers recovered from pretreatment was carried out with the Oxford XMax 50 EDX measuring device from Oxford Instruments in combination with a scanning electron microscope (SEM, Auriga 40 from Zeiss).

2.8 Chemo-enzymatic oxidation

An experimental epoxy resin system based on tetraglycidyl methylene dianiline (TGMDA) was synthesized according to Zotti et al. (2020) and ground into a powder (particle size ≤ 0.6 mm). The TGMDA-based epoxy powder was immersed in 5 M propionic acid/H₂O₂ (95:5) at 60 mL/g, incubated for 48 h at 65 °C with shaking at 230 rpm. The resulting solutions were neutralized with 5 M NaOH and extracted with DCM (1:1). After evaporating the DCM, the precipitate was resuspended in DMSO at a DCM: DMSO ratio of 10:1 based on the original DCM volume. This is referred to extracted epoxy. The remaining powder was filtered, washed with water, and dried overnight at 60 °C. After neutralization and extraction of the extracted epoxy samples, as well as thorough washing of the epoxy powder, any residual acid and H₂O₂ were expected to be completely removed, thereby minimizing the risk of enzyme inactivation in the subsequent step.

10 μL of extracted epoxy was combined with 0.1 U/mg ItL-03, 5 mM CuSO4, and 5 mM ABTS or no mediator in 0.1 M acetate

buffer at pH 4, shaken at 900 rpm at 50 °C. Samples were collected after 2 and 24 h, with bovine serum albumin (BSA) serving as a control. Samples were extracted with DCM (1:1), centrifuged at 13,000 rpm for 5 min, and the organic phase collected for MS analyses.

15 mg of non-treated and pre-treated epoxy powder was incubated with 0.05 U/mg ItL-03 for 5 days under the same settings. Mediators, including ABTS, syringol and (2,2,6,6-tetramethylpiperidin-1-yl)oxidanyl (TEMPO; Thermo Fisher Scientific, Germany), were tested at their optimal pH (Supplementary Figure S8), with TEMPO at pH 4 (Azimi et al., 2016; Wong et al., 2013). After enzymatic treatment, powder was washed with water and dried overnight at 60 °C for FTIR analysis.

2.8.1 Direct electrospray ionization-mass spectrometry (ESI-MS)

ESI-MS analysis was performed via direct injection on an Agilent 6224 ESI-TOF coupled with an Agilent 1200 HPLC. Ionization in positive mode used a 4 kV spray voltage, with a scan range of m/z 110 to 3,200. Flow rate was 0.3 mL/min, with autosampler cooled to 15 °C. Drying gas flow was 10 L/min, nebulizer pressure at 15 psi, and gas temperature at 325 °C. Data were analyzed with MestReNova x64 software (Mestrelab Research S.L.U, Spain). The relative abundance is presented as the mean \pm standard deviation (n=3). Significant differences were determined using one-way ANOVA followed by Tukey's post-hoc test for multiple comparisons, with statistical significance defined as *p < 0.05.

2.8.2 Gas chromatography-mass spectrometry (GC-MS)

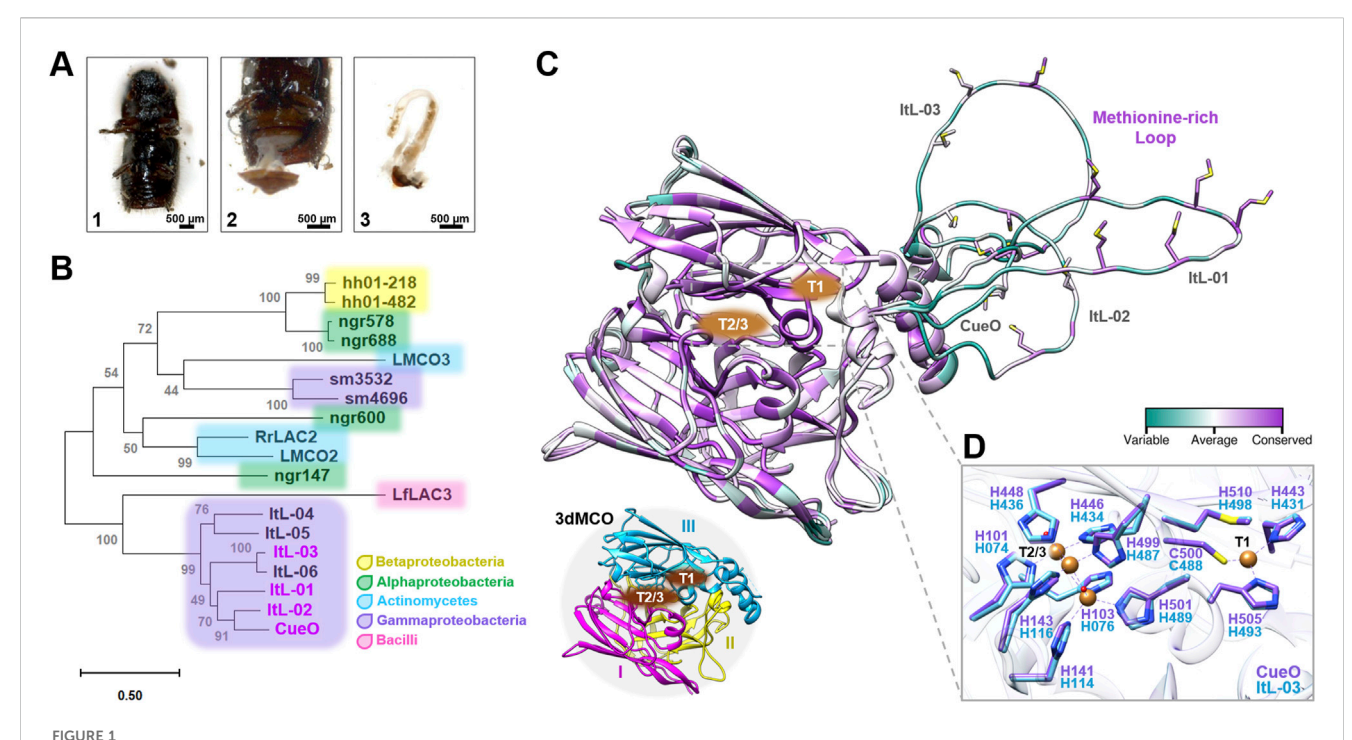
GC-MS analysis was performed on an Agilent GC 7890A GC coupled with an Agilent 5975C VL-MSD. A Thermo Fisher Scientific TG-5MS column (30 m \times 0.25 mm, 0.25 µm) was used. The program started at 80 °C for 1 min, then ramped at 10 °C/min to 300 °C, and held for 10 min. Inlet temperature was 250 °C; helium (5.0) at 1 mL/min with a 1:10 split ratio. Data were acquired in full scan mode (m/z 35–500) with the ion source at 230 °C, and processed using MestReNova x64 software (Mestrelab Research S.L.U, Spain). Data processing and statistical analysis were performed as described in 2.8.1.

3 Results

3.1 Bark beetle metagenome uncovers novel bacterial laccases

European spruce bark beetles colonize and feed on the inner bark layer of trees, a behavior typical of xylophagous beetles that exhibit laccase-like activity in their digestive systems (Christiansen and Bakke, 1988; Geib et al., 2008). This species represents a promising source of enzymes with ligninolytic properties, such as laccases.

The bark beetles were collected in a forest near Hanover, Germany, using pheromone traps, and their gastrointestinal tracts were isolated for microbiota DNA extraction and



Prutative bacterial laccases identified in the gut metagenome of the bark beetle *lps typographus*. (A) Dissection of the bark beetle intestines. The abdomen (1) was opened with sterilized tweezers, (2) and the intestines were removed, (3) and collected in sterile phosphate-buffered saline for DNA extraction. (B) A phylogenetic tree of putative MCOs based on amino acid sequences from beetles and bacteria associated with lignin and synthetic polymer degradation. The accession numbers, UniProt or IMG entries for the sequences used are listed in Supplementary Table S1. (C) The alignment of the 3D structures of CueO and ItL-01-03 shows the conservation of amino acid positions, represented as B-factors. Structural details highlight the copper binding sites (CBSs) T1 and T2/3 sites, and the methionine-rich loop. These MCOs, represented by CueO (PDB: 4NER), consist of three cupredoxin-like domains (3dMCO), labelled I, II, and III. (D) Due to the similarities in CBSs between CueO and ItL-01-03, only CueO (purple) and ItL-03 (blue) are shown.

sequencing (Figure 1A). The assembled metagenomic data, approximately 219 Mbp with a total of 434,200 protein coding genes, were searched for multicopper oxidases (MCOs) or laccases, yielding six putative MCOs designated ItL-01 to ItL-06. However, only ItL-01 to ItL-03 were successfully expressed and produced (Supplementary Figure S1). A phylogenetic tree was constructed based on protein sequences to assess the evolutionary relationships among these laccases, the benchmark laccase CueO from E. coli (Grass and Rensing, 2001; Blattner et al., 1997), eight recognized laccases associated with lignin-rich environments or plant pathogenesis (Hornung et al., 2013; Avison et al., 2000; Trinick, 1980), and three laccases reported to partially degrade polyethylene (PE) (Figure 1B) (Zampolli et al., 2023; Zhang Y. et al., 2023). Phylogenetic analysis revealed that these MCOs are predominantly affiliated with the phylum Pseudomonadota, with few belongings to Actinomycetota and Bacillota, aligning with the taxonomic classification of bacterial laccases in the LccED database (Gräff et al., 2020). ItL-01 to ItL-06 exhibit over 60% sequence similarity to CueO, while the other laccases have identities below 40% (Supplementary Table S1).

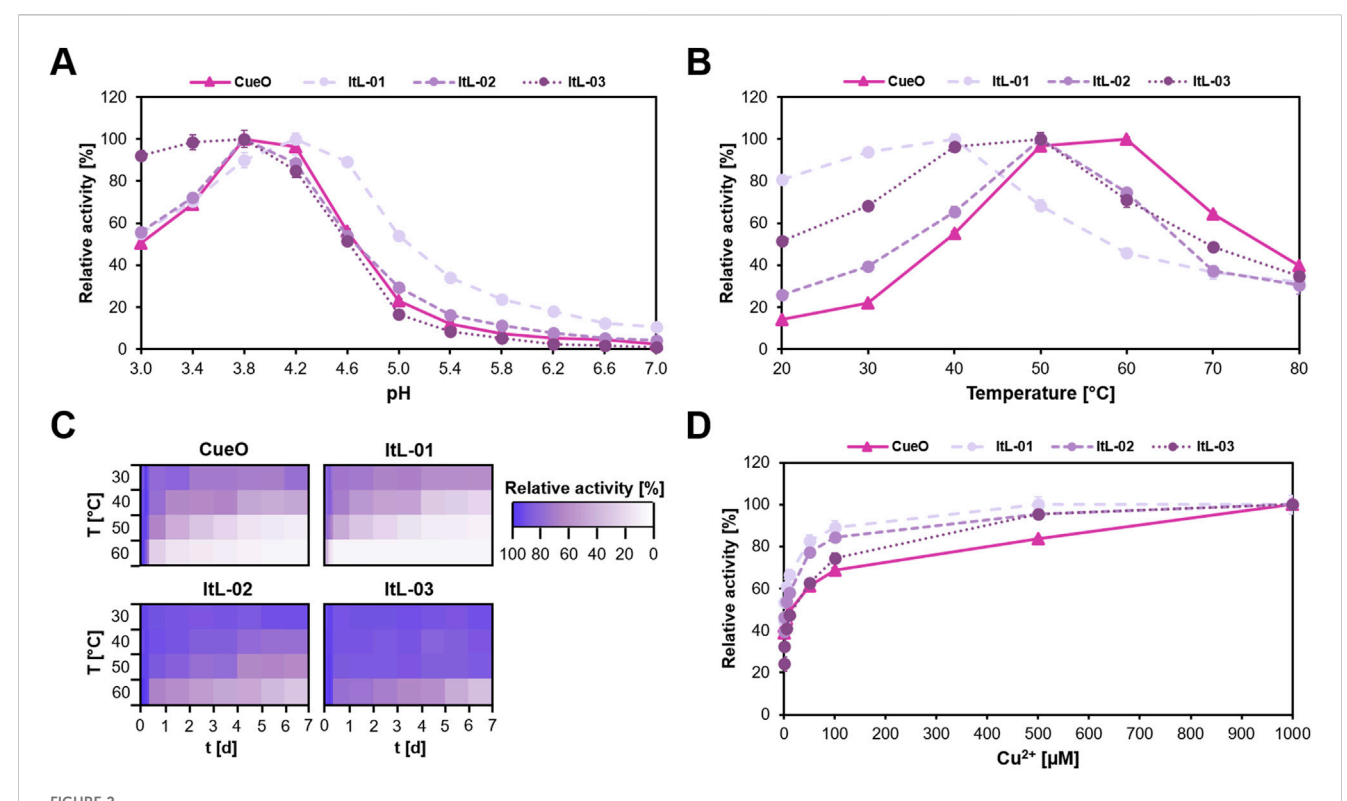
The 3D structural analysis indicates that these laccases are typical three-domain MCOs (3dMCO), with highly conserved regions near the two copper binding sites (CBSs) at the T1 and T2/T3 centers (Figure 1C). The T1 copper ion is located in the third domain, where the substrate is oxidized, while the T2 and T3 copper

ions interface between the first and third domains, where dioxygen reduction takes place (Gräff et al., 2020). In contrast, methionine-rich loops near the T1 site, are considerably variable. In fact, the methionine residues themselves are quite conserved. These methionines are thought to facilitate the recruitment and transport of copper (Contaldo et al., 2024).

Crystals of CueO (PDB 4NER; Komori et al., 2014), with a resolution of 1.60 Å and containing copper (II) ions, were used to map CBSs with ItL-03, showing high similarity and conservation among MCOs, predominantly with histidine residues (His) (Figure 1D). Given the highly conserved topology of CBSs, the methionine-rich loops may influence enzyme specificity and reactivity, e.g., regulating substrate access and stabilizing substrates (Borges et al., 2020).

3.2 Biochemical characterization identifies thermostable laccases functioning at low pH

Recombinant enzymes CueO and ItL-01-03 were produced and purified via affinity chromatography, yielding predicted molecular weights of 50-60 kDa (Supplementary Figure S1). ABTS (2,2'-azinobis (3-ethylbenzothiazoline-6-sulfonic acid)), a common mediator in laccase/mediator systems and a typical substrate for laccases (Hilgers et al., 2018), was used to measure radical formation at 420 nm to investigate enzyme characteristics.



Biochemical characteristics of CueO and ItL-01–03, determined using ABTS, highlight their optimal enzyme activity and stability. (A) pH profile: the enzymes preferred low pH and reached their maximum activity at pH 4.0. (B) Temperature profile: each enzyme exhibited a distinct temperature stability, within the mesophilic range of 30 °C–60 °C. (C) Thermostability: most enzymes retained their activity for only a few hours, losing nearly 80% within a day at elevated temperatures, while ItL-02–03 maintained over 60% activity at 50 °C for a week. (D) Effect of copper ions (Cu^{2+}): the activity of laccases significantly increases with higher Cu^{2+} when supplemented during enzymatic reactions. Error bars indicate the standard deviation (n = 3). The standard deviation in 'C' was below 6%. Buffer preference is shown in Supplementary Figure S2.

The bacterial laccases showed a preference for the acidic pH range, maintaining over 50% activity between pH 3.0 and 4.6 (Figure 2A). ItL-01 reached a pH maximum of 4.2, while CueO, ItL-02, and ItL-03 peaked at pH 3.8. Particularly, ItL-03 retained over 90% activity between pH 3.0 and 3.8, indicating pronounced acidophilic nature. Since the optimal pH range for these enzymes was similar, acetate buffer at pH 4.0 was selected for further characterization (Supplementary Figure S2).

Temperature profiles and thermostability were assessed by incubating enzymes at 30 °C–60 °C for 7 days. The bacterial laccases exhibited moderate optimal temperatures (T_{opt}) (Figure 2B). ItL-01 had a T_{opt} of 40 °C, retaining over 80% activity after 10 h (Figure 2C). CueO exhibited the highest T_{opt} at 60 °C, but experienced a 30% drop-in activity after 10 h and nearly lost all activity after 3 days. ItL-02 and ItL-03 shared the same T_{opt} of 50 °C. While ItL-02 retained 80% activity at its T_{opt} after 2 days, ItL-03 sustained this level even after 7 days (Figure 2C), making it the most thermophilic and thermostable enzyme in this study.

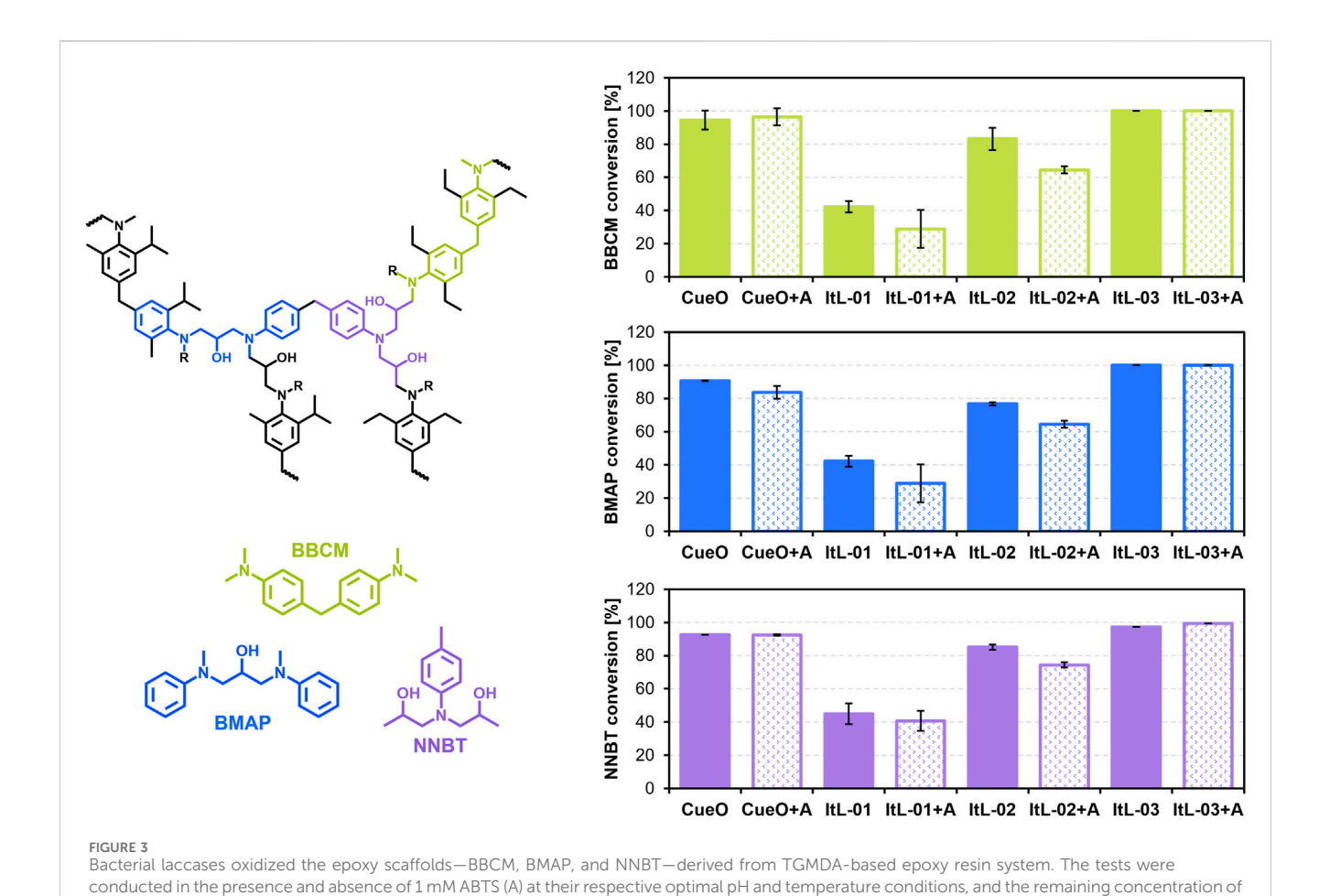
To ensure proper folding, $0.25~\mu\mathrm{M}$ CuSO₄ was supplied during enzyme production. Supplementing additional Cu²⁺ into the reactions resulted in a gradual increase in laccase activity (Figure 2D). The steady-state kinetics of the laccases were determined with respect to ABTS, revealing similar catalytic turnover values (Supplementary Table S3). Among all, ItL-03 exhibited the highest catalytic turnover ($k_{\rm cat}=3.04~{\rm min}^{-1}$) but had relatively high $K_{\rm m}$ value of 7.76 mM. However, in terms of

catalytic efficiency ($K_{\rm cat}/K_{\rm m}$), ItL-03 outperformed the other laccases with a value of 0.39 min⁻¹ mM⁻¹. Based on these initial characterizations, the laccases were further evaluated for their catalytic properties toward epoxy model building blocks.

3.3 Laccases can oxidize epoxy resin building blocks

The laccases were tested for their ability to oxidize bis(4-dimethylamino-cyclohexyl) methane (BBCM), 1,3-bis(methyl (phenyl)amino) propan-2-ol (BMAP), and N, N-bis(2-hydroxypropyl)-p-toluidine (NNBT) (Figure 3). These substrates contain key resin motifs, including a tertiary amine found in a recognized high-performance tetraglycidyl methylene dianiline (TGMDA)-based epoxy resin system used in the aerospace sector (Zotti et al., 2020), and serve as models to study enzyme mechanisms on C–N bonds in the original polymer.

Laccase activity on these epoxy scaffolds was monitored after 2 h using liquid chromatography-mass spectrometry (LC-MS) (Supplementary Figure S4), with quantification based on calibration curves (Supplementary Figure S5). The laccases exhibited comparable activity levels across the different substrates. ItL-03 showed the highest activity, converting almost all of the three substrates BBCM, BMAP, and NNBT within 2 h (Figure 3), and achieving 80% conversion after just 30 min (Supplementary Figure S6). This was followed closely by CueO,



the epoxy substrate after 2 h was measured using LC-MS (Supplementary Figure S4). The initial observation (t₀) defined the starting amount of epoxy, set at 100%. The conversion rate was calculated by subtracting the percentage of remaining epoxy from 100%. Error bars indicate the standard deviation

ItL-02, and ItL-01, with conversions of approximately 90%, 80%, and 40%, respectively. LC-MS analysis indicated possible N-dealkylation activity of the enzymes (Supplementary Figure S7).

(n = 3). Supporting data can be found in Supplementary Figures S4-S7.

Given that laccase activity could be enhanced by a mediator, the effect of ABTS (A) were evaluated. The presence of ABTS only slightly affected the enzymes' activity, resulting in either a marginal decrease or nearly the same level of activity (Figure 3, +A). This is likely because the small model substrates can access the enzyme's active site directly, making a mediator unnecessary. Among the bacterial laccase candidates, ItL-03 emerged as the most effective in oxidizing the epoxy scaffolds, prompting further analysis of its efficacy on cured epoxy.

The activity of laccase ItL-03 was further investigated with additional mediators, syringol and guaiacol. The optimal pH and buffer preferences for each mediator were determined (Supplementary Figure S8), and the specific activities of ItL-03 with ABTS, syringol, and guaiacol were assessed (Supplementary Figure S9A). ItL-03/syringol exhibited the highest activity, approximately four times greater than that of ABTS, while guaiacol showed relatively low specificity. The optimal concentration of copper was further determined to be 5 mM for ItL-03 activity (Supplementary Figure S9B).

The activity of ItL-03 on NNBT with mediators was evaluated (Supplementary Figure S10). ItL-03/guaiacol oxidized NNBT more rapidly than with ABTS, achieving 90% conversion in 30 min,

although similar conversion levels were reached after 2 hours. Since guaiacol is a phenolic mediator similar to syringol but with a slightly lower oxidation potential, and achieves comparable NNBT conversion levels to ABTS, it was excluded from further investigation.

Initial assays on eCFRPs, however, did not result in any observable changes in physical appearance or mass loss due to enzymatic activity. Therefore, pre-treatment was investigated to determine its potential to enhance enzyme access to resulting oligomers or reaction intermediates.

3.4 Propionic acid-peroxide recovers clean carbon fibers and decomposes epoxy based CFRPs

Conventionally, the European standard (DIN EN 2564:2018) employs concentrated sulfuric acid and 30% hydrogen peroxide ($\rm H_2O_2$) to treat CFRPs at high temperatures (160 °C–260 °C) to determine fiber, resin, and void contents. Due to high corrosiveness and toxicity, alternative organic acids—formic acid (FA), acetic acid (AA), propionic acid (PA), lactic acid (LA), malic acid (MA), tartaric acid (TA), citric acid (CA)—combined with $\rm H_2O_2$ were selected for eCFRP pre-treatment. These acids are less toxic, derived from renewable sources, and biodegradable.

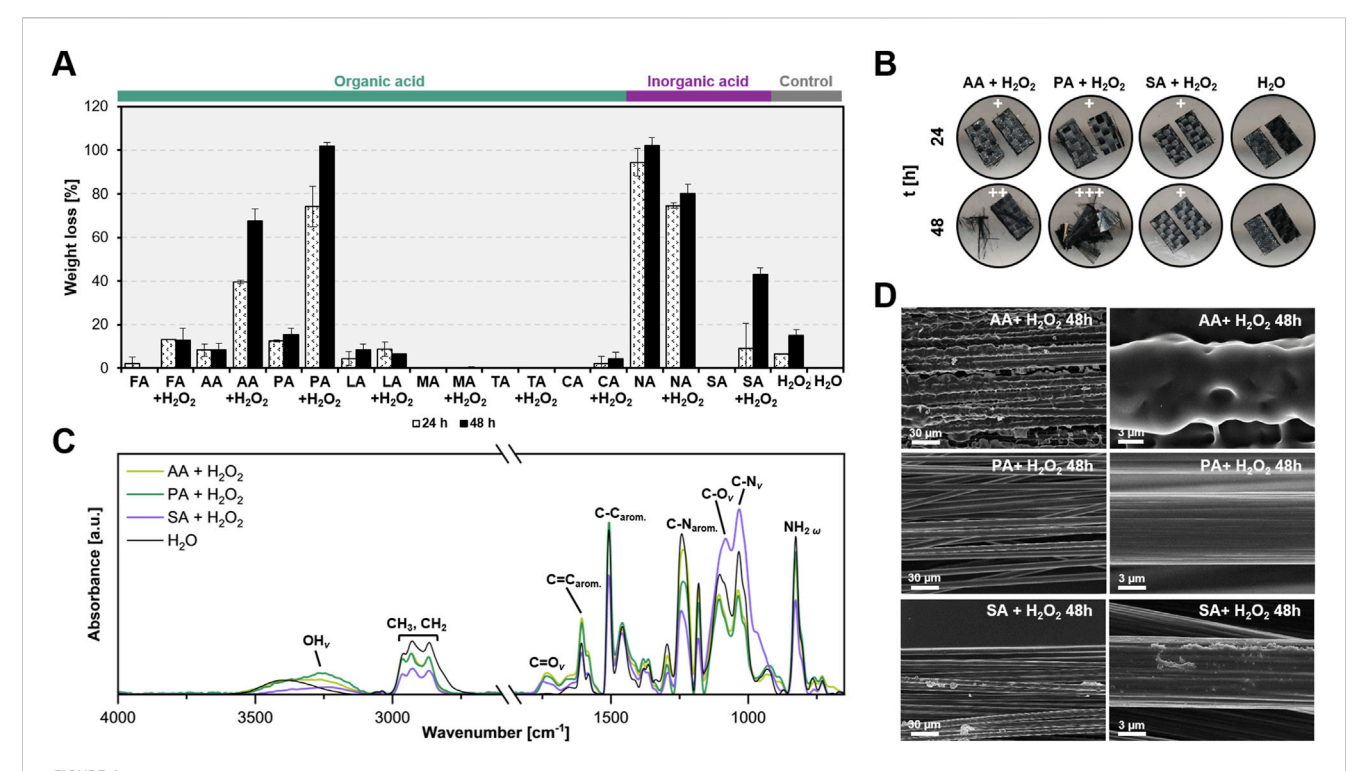


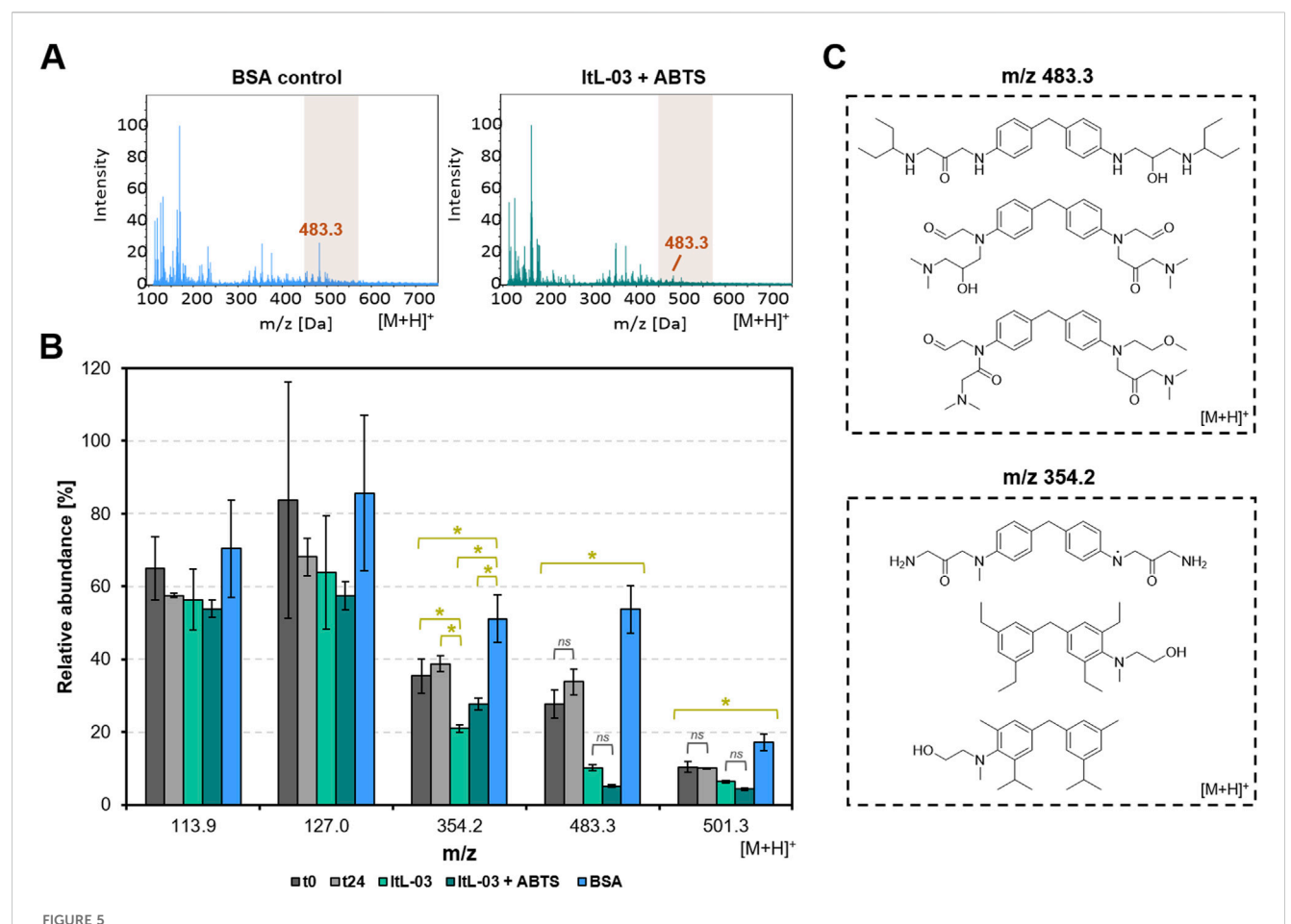
FIGURE 4 Organic acid treatments are effective in decomposing epoxy polymers and recovering clean carbon fibers. (A) Weight loss of the resin mass in eCFRPs treated with organic acids, with and without hydrogen peroxide (H_2O_2) , was compared to inorganic acids and controls (H_2O_2) . The acids tested included formic acid (FA), acetic acid (FA), propionic acid (FA), lactic acid (FA), malic acid (FA), trataric acid (FA), citric acid (FA), and sulfuric acid (FA). Composites were incubated in a 95:5 acid-to-peroxide ratio at a 5 M, 65 °C, and 200 rpm for 24 and 48 h. Error bars indicate the standard deviation (n = 3). (B) Morphological changes in the composites after 24 and 48 h of pre-treatment. +, ++, and +++ represent the degree of carbon fiber exposure, ranging from low to high. (C) FTIR analysis of the 8-h pre-treatment of eCFRPs. The corresponding functional groups are indicated. V denotes stretching, while W denotes wagging. (D) SEM images of the eCFRPs after 48-h treatments. Scale bars indicate size in micrometers (V). Supporting data can be found in Supplementary Figures S11-S15.

Diglycidyl ether of bisphenol A (DGEBA)-based composites were treated at 60 °C for 24 and 48 h in a 5 M acidic-peroxide mixture with a 95:5 ratio. This specific ratio minimizes damage to carbon fibers due to the limited amount of H₂O₂ (Das et al., 2018). Their remaining weights, after pre-treatment, were calculated to evaluate the efficacy of different acids. All treatments with H₂O₂, except for NA, exhibited higher resin decomposition than those without (Figure 4A). This highlights the importance of H₂O₂ in the reaction mechanism, probably due to the in-situ formation of peracids. AA- and PA-H₂O₂ achieved 40% and 80% epoxy resin weight loss after 24 h, respectively, with the latter capable of completely removing the resin after 48 h. Using 9 M AA- and PA-H₂O₂ enabled effective depolymerization within 8 h (Supplementary Figure S11). Conversely, high molecular weight organic acids (LA, MA, TA, CA) and SA showed minimal oxidative activity towards the composites (Figure 4A).

Carbon fibers (CFs) became visible in composites treated with PA- $\mathrm{H_2O_2}$ after 48 h (Figure 4B; Supplementary Figure S12). Scanning electron microscopy (SEM) images revealed clean and elongated CFs from the PA- $\mathrm{H_2O_2}$ treatment comparable to those treated under the European protocol (Figure 4D; Supplementary Figure S13). Energy Dispersive X-ray (EDX) analysis confirmed that CFs recovered after PA- $\mathrm{H_2O_2}$ predominantly contained carbon (C), with negligible oxygen content likely due to manufacturing impurities (Supplementary Figure S14).

Fourier Transform Infrared Spectroscopy (FTIR) analysis was performed to examine changes in functional groups following pretreatments. The C=C aromatic band (around 1,600 cm⁻¹) was evident in all epoxy composites, while the C=O stretching band (around 1,750 cm⁻¹) appeared only in samples subjected to acidperoxide pre-treatment, indicating possible oxidation (Figure 4C). AA- and PA-H₂O₂ exhibited higher peak intensities in the C=C region than SA-H₂O₂, possibly due to the formation of carbonyls. Epoxy functional groups (e.g., C-N stretching in primary aliphatic and aromatic amines, around 1,030 cm⁻¹ and 1,240 cm⁻¹ respectively) significantly decreased in the AA- and PA-H₂O₂ treated samples (Figure 4C). The stretching peaks of OH and C=O bonds in epoxy treated with organic acid-H₂O₂ were more pronounced than those in SA-H₂O₂, which was more effective at converting C-N in aromatic amines to C-N in primary amines. This suggests that organic and inorganic acids target different functional groups. Additionally, H2O2 proved to be a key component in acid pre-treatment, contributing to epoxy decomposition by primarily altering epoxy functional groups, as shown in Supplementary Figure S15. This suggests that combining H₂O₂ with organic acids enhances their efficiency, making them comparable to SA-H₂O₂ treatment.

These findings demonstrate that $PA-H_2O_2$ pre-treatments effectively promote epoxy mass loss, likely accompanied by a reduction in cross-link density, while also offering the advantage



ESI-MS analysis of extracted epoxy from chemo-enzymatic treatment using PA- H_2O_2 and laccase ItL-03 on TGMDA-based epoxy. (A) ESI-MS spectrum obtained via direct injection in positive mode, showing the activity of ItL-03 with ABTS and BSA control after 24 h. m/z 483.3 was mostly absent in the laccase sample but remained present in the control. (B) The relative abundance of m/z values of interest from the same experiment in 'A' is shown, including other samples. The spectra were normalized using the m/z value at 163.9 as a reference peak. t_0 and t_{24} represent controls without enzyme at the beginning and end of the incubation period. Error bars represent the standard deviation (n = 3). Statistical differences were analyzed using one-way ANOVA with Tukey's HSD post-hoc test (*p < 0.05). Non-significant pairs are indicated as ns (p > 0.05). (C) The proposed compounds with m/z values of 483.3 and 354.2 may undergo enzymatic conversion. Adduct formation corresponding to the protonated molecular ions ([M + H]+) has been considered when predicting their structures. Supporting data can be found in Supplementary Figures S16-S18.

of lower environmental risks. This pre-treatment allows for the recovery of clean CFs, which could potentially be reused.

3.5 PA-H₂O₂ enhances laccase activity, enabling further partial modification of TGMDA-based epoxy resin system

The $PA-H_2O_2$ pre-treatment effectively depolymerized the epoxy matrix of the DGEBA-based composite and recovered clean CFs. While CFs can be retrieved using the pre-treatment, it is important to determine whether laccase ItL-03 can further modify the pre-treated polymeric matrix and break down the soluble oligomers generated during pre-treatment into a more defined educt for downstream processing.

To evaluate the potential for enhanced bio-based recycling through chemo-enzymatic oxidation, an experimental epoxy resin system was used, synthesized from TGMDA amine epoxy precursor and the di-amine hardeners 4,4'-methylenebis (2,6-diethylaniline)

(MDEA) and 4,4'-methylenebis (2-isopropyl-6-methylaniline) (M-MIPA) (Zotti et al., 2020). TGMDA-based epoxy was selected over the composite, as the CFs were no longer considered, and it also enabled the investigation on this amine-cured epoxy. Following PA- $\rm H_2O_2$ pre-treatment of the epoxy powder, the resulting solution was neutralized and extracted, referred to as 'extracted epoxy'. This extracted epoxy was subsequently introduced to ItL-03, and the resulting samples were analyzed using electrospray ionization-mass spectrometry (ESI-MS) via direct injection and gas chromatographymass spectrometry (GC-MS).

ESI mass spectra revealed that the PA- H_2O_2 treatment effectively depolymerized epoxy resins into several small compounds within mass-to-charge ratio (m/z) ranges of 150–200 and 300-500 (Supplementary Figure S16). However, after 24 h of treatment with ItL-03, the ions at m/z 483.3 were present but at a relatively low abundance, especially with the addition of the mediator ABTS, when compared to the BSA and buffer controls (t_0 and t_{24}) (Figure 5A). Additionally, ions at m/z 354.2 and 501.3 were detected at lower intensities in the laccase

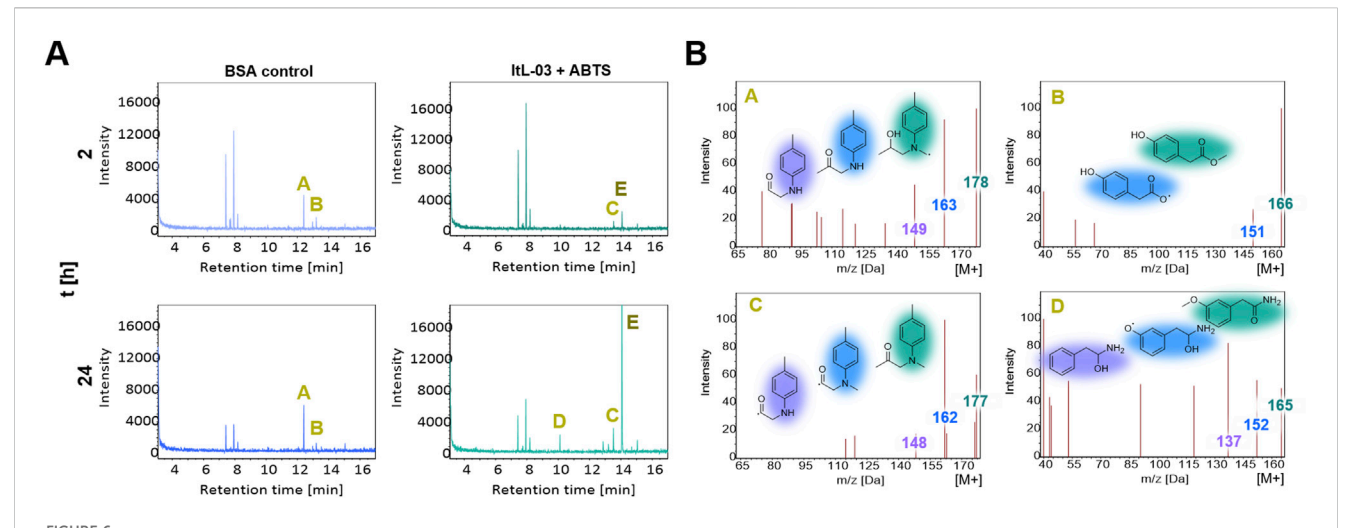


FIGURE 6 GC-MS analysis of extracted epoxy from chemo-enzymatic treatment using PA- H_2O_2 and laccase ItL-03 on TGMDA-based epoxy. (A) GC-MS chromatogram presenting the activity of ItL-03 with ABTS, compared to BSA control after 2 and 24 h. The peaks of interest are indicated with A-E. (B) Proposed species derived from the amine-cured epoxy that may be oxidized by ItL-03, based on mass spectra of peaks A and B, with additional peaks C and D emerging in the ItL-03/ABTS samples after 2 and 24 h. Chemical structures are colour-highlighted to indicate different fragment ions m/z. Supporting data can be found in Supplementary Figure S19-S21 and additional species related to peaks A-E are presented in Supplementary Figures S22-S24.

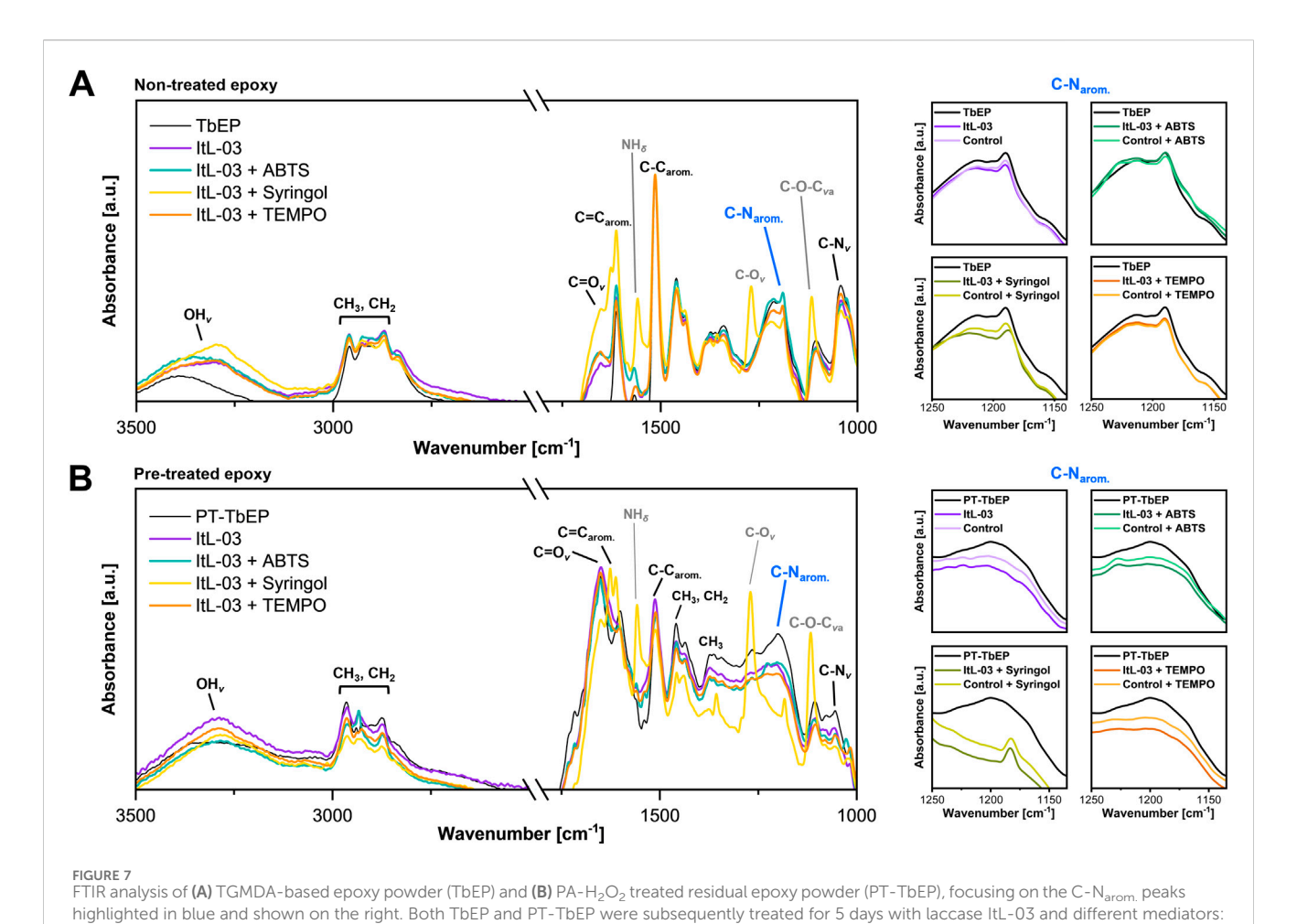
samples, regardless of ABTS presence (Figure 5B; Supplementary Figure S17). The reduced abundance of ions at m/z 354.2 and 483.3 in the presence of laccase ItL-03 suggests potential conversion or oxidation by the enzyme. While these trends are consistent across enzyme-treated samples and controls, some results were not statistically significant, such as those for peaks at m/z 113.9 and 127.0. Figure 5C proposes potential structures considering adduct formation, as the molecule was detected as a protonated ion ([M + H] $^+$).

GC-MS chromatograms indicated that the PA-H₂O₂ treatment decomposed cured epoxy resins into compounds with retention times of 7-9 and 12-14 min, as evidenced by distinct peaks A and B in BSA and control samples (Figure 6A; Supplementary Figure S19). Notably, peak B was absent in samples treated with ItL-03, while peak A was additionally absent when combined with ABTS (Supplementary Figure S20). In ItL-03/ABTS samples, peak C appeared, and an additional peak D was detected after 24 h (Figure 6A). Peaks A and B, attributed to m/z 178 and 166, respectively, may have been oxidized by laccase and could originate from NNBT or fractions of the amine-cured epoxy (Figure 6B). The ion at m/z 178 could possibly have been deprotonated to form the ion at m/z 177, corresponding to Peak C, as they exhibited similar ionization patterns. Alternatively, these ions may represent distinct molecules with nearly identical masses, such as the m/z pairs of 166-165 proposed for peaks B and D. Additional species at m/z 178, 177, 166, and 165 are proposed in Supplementary Figure S22, S23. Furthermore, the ItL-03/ABTS treatment produced a prominent peak E, corresponding to m/z 144 (Supplementary Figure S24). This peak is likely a fragment of ABTS, as it exhibited ionization patterns consistent with its mass fraction. The results from mass spectrometry suggest that the laccase has the potential to further act on a few by-products generated after pre-treatment, which could help improve downstream applications and facilitate product recovery. However, the structural assignments

are tentative and require further confirmation by MS/MS or nuclear magnetic resonance (NMR).

Since the PA- $\rm H_2O_2$ treatment of TGMDA-based epoxy powder (TbEP) from the same batch did not completely decompose the amine epoxy, any remaining epoxy powder was also tested for laccase ItL-03 activity. Before enzyme treatment, FTIR spectra showed distinct band patterns between non-treated (TbEP) and pre-treated (PT-TbEP) epoxy powders, indicating that PA- $\rm H_2O_2$ treatment induced changes in the functional groups of epoxy resins (Supplementary Figure S25). The C=O stretching band (around 1,750 cm⁻¹) was present only in PT-TbEP and absent in TbEP, further confirming the oxidative effect of the pre-treatment on the DGEBA-based composites (Figure 4C).

Subsequently, both TbEP and PT-TbEP were subjected to enzymatic treatment with ItL-03 in the presence of different mediators: ABTS, syringol, and TEMPO. For TbEP samples, there was a significant change in the peak intensity of the C-N stretching associated with aromatic amines (1,210-1,180 cm⁻¹) in the presence of enzyme (Figure 7A). However, this effect resembled that of the BSA control, suggesting that the band shifts may be due to water incubation rather than enzymatic activity (Supplementary Figure S26). Epoxy resin is prone to absorb water and swell, potentially leading to a weakening of its mechanical integrity (Walter et al., 2013). This is not the case for the ItL-03/DMP, which exhibited slight changes that differed from the control. For PT-TbEP, epoxy functional groups, such as C-N stretching in aromatic (around 1,200 cm⁻¹) and primary (1,085-1,050 cm⁻¹) amines, were less pronounced in the samples treated with ItL-03 compared to those without (PT-TbEP) (Figure 7B). A more significant effect was observed in the presence of mediators (Supplementary Figure S27). This suggests that pre-treatment facilitates enzyme access to the embedded epoxy functional groups in the polymer, particularly the amine functionalities, allowing for further oxidation.



ABTS, syringol, and TEMPO. The samples labelled "TbEP" and "PT-TbEP" were not subjected to enzyme treatment and the control refers to the BSA incubation of the epoxy instead of laccase. The corresponding functional groups are indicated. ν—stretching; νa—asymmetric stretching; δ—deformation. Other functional group peaks, in comparison to BSA, are shown in Supplementary Figures S26, S27.

4 Discussion

In recent years, the search for sustainable waste management solutions has increasingly focused on biodegradation of recalcitrant synthetic polymers like epoxy resins. To date, no microorganism or enzyme has been clearly shown to effectively degrade cured epoxy polymers (PAZy database; Buchholz et al., 2022). Our study represents an early step forward by demonstrating that a two-step process involving PA-H₂O₂ pretreatment followed by laccase ItL-03 can partially modify TGMDA-based epoxy resins and act on certain low-molecular-weight (LMW) products.

The studies by Dolz et al. (2022) represent one of the first investigations into NNBT, derived from an amine epoxy resin system, demonstrating that it can be cleaved by unspecific peroxygenases (UPOs) through N-dealkylation. Our study shows that bacterial laccases can also convert NNBT and expand the scope to include other tertiary amine epoxy substrates, BBCM and BMAP, through an N-dealkylation activity.

Laccases can catalyze the oxidation of epoxy substrates containing tertiary amines, but have minimal effect on cured epoxy polymer, without pre-treatment. The steric hindrance from the densely packed, cross-linked structure likely limits enzyme access to certain regions within the molecule (Escayola et al., 2024; Pinter et al., 2012). This limitation can be overcome through pre-treatment with propionic acid (PA) and H₂O₂. The mechanism of the pre-treatment for decomposing cross-linked epoxy primarily involves the formation of a peracid through the reaction of a COOH-containing acid with H₂O₂ (Luukkonen and Pehkonen, 2017). These unstable peracids initially generate acyloxyl (CH₃CH₂COO·) and hydroxyl (·OH) radicals. The acyloxyl radicals oxidize C–OH groups to carbonyl (C=O) groups, which then induce cleavage of C–N bonds, disrupting the cross-linked network. Hydroxyl radicals primarily oxidize hydroxyl groups to carbonyls but are less effective at breaking other bonds (Das et al., 2018).

Recycled carbon fibers obtained using ASTM D3171 (standard test methods for constituent content of composite materials) with concentrated sulfuric acid and $\rm H_2O_2$ (used at a 1:1 or 2:1 v/v ratio) retain 50%–80% of the key physical and mechanical properties of the original material, including tension, compression, flexure, and short beam shear (Feraboli et al., 2011). When $\rm H_2O_2$ is omitted, retention increases to approximately 90% (Nan et al., 2025). Therefore, recovered carbon fibers treated with the less corrosive PA- $\rm H_2O_2$ may retain an even higher proportion of these properties, making them potential for reuse. However, this still needs to be experimentally confirmed.

Laccase appeared to target amine functionalities more effectively following pre-treatment, leading to additional modifications of C-N, CH₃, CH₂, and C-O-C linkages. This suggests that pre-treatment creates reactive sites on the polymer surface, similar to natural conditions where factors such as microbial colonization and seawater can promote epoxy oxidation and hydrolysis (Dang and Lovell Charles, 2015; Da Costa et al., 2018), mimicking pretreatment that prepares substrates for enzyme activity. Bacteria and fungi colonizing epoxy polymers (Gu et al., 1997; Wang et al., 2016) often possess oxidoreductases (EC1), such as laccases, peroxidases, monooxygenases, dehydrogenases (Kumar and Chandra, 2020; Naveed et al., 2025; Padayachee et al., 2020), which have been reported to have the potential to partially modify non-hydrolysable plastics like polyethylene (PE), polypropylene (PP), polystyrene (PS), and polyvinyl chloride (PVC) (Chow et al., 2023; Mohanan et al., 2020).

Other studies have shown that combining pre-treatment with enzymes enhances depolymerization of non-hydrolysable polymers. Branson et al. (2023) demonstrated that glycolyzing polyether polyurethane foams at 200 °C with diethylene glycol (DEG) and 1% tin (II)-2-ethylhexanoate produced LMW dicarbamates, which were hydrolyzed into aromatic diamines with urethanase UMG-SP-2, achieving a 65% conversion in 24 h. Similarly, pre-treating LMWPE with m-chloroperoxybenzoic acid (mCPBA) and ultrasonication improved enzyme accessibility, resulting in approximately 27% polymer conversion and releasing mediumchain products, such as aliphatic carboxylic acids (Oiffer et al., 2024).

Combining PA-H₂O₂ treatment with laccase ItL-03 has shown promise in enhancing the modification of epoxy polymers compared to using enzymes alone. Laccase is likely more effective at oxidizing soluble oligomers generated during pre-treatment than at modifying pre-treated, cured epoxy. Although pre-treatment improves enzyme accessibility and facilitates reactions with functional groups on the polymer surface, it is hypothesized that the enzyme primarily oxidizes newly generated surface functional groups rather than continuing to cleave the polymer backbone, as decomposition of the pre-treated epoxy after enzyme treatment is negligible and cannot be detected by weight loss or conversion rate measurements. These modifications are largely confined to the surface, and it remains unclear whether the enzymes induce further chain scission within the bulk polymer or act only on newly exposed surface regions. Further studies are needed to elucidate this mechanism. The current extent of polymer matrix alteration by the enzyme may not yet meet industrial requirements. Nevertheless, the selectivity of these enzymes toward byproducts formed after pre-treatment offers advantages for potential downstream applications, indicating a promising area for further development to improve enzyme-mediated processes industrial use.

Expanding enzyme screening to include various epoxy types, such as secondary amines (R–NH– CH_2 –R'), carboxyl esters (R–(C=O)–O–R'), ethers (R–O–R'), and thiol (R–S–R') linkages (Rashid et al., 2024), and larger model substrates would improve our understanding of enzymatic mechanisms, particularly for bacterial laccases with high redox mediators. Though propionic acid can be biologically produced through microbial fermentation, such as with *Propionibacterium freudenreichii* and *P. acidipropionici* (Gonzalez-Garcia et al., 2017; Ranaei et al., 2020), and recovered for reuse

through methods like microchannel distillation (Singh et al., 2021; Lu et al., 2023), minimizing pre-treatment is important to ensure adequate enzyme access while enhancing process sustainability.

Effective recycling of epoxy resins necessitates a multifaceted approach that incorporates physical, chemical, and enzymatic methods. While significant challenges remain, our study offers an innovative preliminary biological concept for epoxy waste management. Continued research will be essential to transform this potential into practical, scalable recycling methods.

Data availability statement

The datasets presented in this study can be found in online repositories. The names of the repository/repositories and accession number(s) can be found in the article/Supplementary Material.

Ethics statement

The manuscript presents research on animals that do not require ethical approval for their study.

Author contributions

SW: Conceptualization, Formal Analysis, Investigation, Methodology, Validation, Visualization, Writing – original draft, Writing – review and editing. AS: Data curation, Formal Analysis, Investigation, Methodology, Writing – review and editing. LK: Formal Analysis, Investigation, Resources, Writing – review and editing. CC: Formal Analysis, Writing – review and editing. AM: Resources, Writing – review and editing. AL: Resources, Writing – review and editing. PP-G: Conceptualization, Methodology, Supervision, Writing – review and editing. WS: Conceptualization, Funding acquisition, Supervision, Writing – review and editing.

Funding

The author(s) declare that financial support was received for the research and/or publication of this article. This work was supported by the Office of Naval Research Global (ONRG) under the Global-X project (Grant No. N62909-21-1-2025) and by the German Federal Ministry of Education and Research (BMBF) under the LipoBiocat2 project (Grant No. 031B1342B).

Acknowledgments

We would like to thank Phillip Schlottau from the Department of Physics, for the assistance with laser cutting on epoxy. We acknowledge Elke Wölken from the Microscopy Department, with support from SEM, as well as the Core Facility Mass Spectrometry, part of the Technology Platform Mass Spectrometry, particularly Gaby Graack and Erik Mordhorst, for their support with mass spectrometric analysis. We extend our

thanks to Siraphat Weerathaworn from the Institute of Physical Chemistry for FTIR assistance. All contributors are from the University of Hamburg. The epoxy substrate BMAP was kindly provided by Prof. Nigel Scrutton from the Manchester Institute of Biotechnology at The University of Manchester (UK). We are grateful to Max Kolb from Airbus Defense and Space GmbH, X-Labs (Munich, Germany) for performing SEM/EDX analysis on the pre-treated CFRPs.

Conflict of interest

Author CC was employed by Airbus Defence and Space GmbH. The remaining authors declare that the research was conducted in the absence of any commercial or financial relationships that could be construed as a potential conflict of interest.

Generative AI statement

The author(s) declare that no Generative AI was used in the creation of this manuscript.

References

Aamir, M., Tolouei-Rad, M., Giasin, K., and Nosrati, A. (2019). Recent advances in drilling of carbon fiber–reinforced polymers for aerospace applications: a review. *Int. J. Adv. Manuf. Technol.* 105, 2289–2308. doi:10.1007/s00170-019-04348-z

Abramson, J., Adler, J., Dunger, J., Evans, R., Green, T., Pritzel, A., et al. (2024). Accurate structure prediction of biomolecular interactions with AlphaFold 3. *Nature* 630, 493–500. doi:10.1038/s41586-024-07487-w

Ahmad, H., Markina, A. A., Porotnikov, M. V., and Ahmad, F. (2020). A review of carbon fiber materials in automotive industry. *IOP Conf. Ser. Mater. Sci. Eng.* 971, 032011. doi:10.1088/1757-899x/971/3/032011

Armougom, F., Moretti, S., Poirot, O., Audic, S., Dumas, P., Schaeli, B., et al. (2006). Expresso: automatic incorporation of structural information in multiple sequence alignments using 3D-Coffee. *Nucleic Acids Res.* 34, W604–W608. doi:10.1093/nar/gkl092

Author anonymous (2018). Database resources of the national center for biotechnology information. *Nucleic Acids Res.* 46, D8–D20. doi:10.1093/nar/gks1189

Avison, M. B., Von Heldreich, C. J., Higgins, C. S., Bennett, P. M., and Walsh, T. R. (2000). A TEM-2beta-lactamase encoded on an active Tn1-like transposon in the genome of a clinical isolate of Stenotrophomonas maltophilia. *J. Antimicrob. Chemother.* 46, 879–884. doi:10.1093/jac/46.6.879

Azimi, M., Nafissi-Varcheh, N., Mogharabi, M., Faramarzi, M., and Aboofazeli, R. (2016). Study of laccase activity and stability in the presence of ionic and non-ionic surfactants and the bioconversion of indole in laccase-TX-100 system. *J. Mol. Catal. B Enzym.* 126, 69–75. doi:10.1016/j.molcatb.2016.02.001

Bassanini, I., Ferrandi, E. E., Riva, S., and Monti, D. (2021). Biocatalysis with laccases: an updated overview. *Catalysts* 11, 26. doi:10.3390/catal11010026

Blattner, F. R., Plunkett, G., 3rd, Bloch, C. A., Perna, N. T., Burland, V., Riley, M., et al. (1997). The complete genome sequence of *Escherichia coli* K-12. *Science* 277, 1453–1462. doi:10.1126/science.277.5331.1453

Bolger, A. M., Lohse, M., and Usadel, B. (2014). Trimmomatic: a flexible trimmer for illumina sequence data. *Bioinformatics* 30, 2114–2120. doi:10.1093/bioinformatics/btu170

Bombardier (2017). Projected number of passenger aircraft to be removed from service between 2017 and 2036, by region. Hamburg, Germany: Statista.

Boratyn, G. M., Schäffer, A. A., Agarwala, R., Altschul, S. F., Lipman, D. J., and Madden, T. L. (2012). Domain enhanced lookup time accelerated BLAST. *Biol. Direct* 7, 12. doi:10.1186/1745-6150-7-12

Borges, P. T., Brissos, V., Hernandez, G., Masgrau, L., Lucas, M. F., Monza, E., et al. (2020). Methionine-rich loop of multicopper oxidase McoA follows open-to-close transitions with a role in enzyme catalysis. *ACS Catal.* 10, 7162–7176. doi:10.1021/acscatal.0c01623

Branson, Y., Söltl, S., Buchmann, C., Wei, R., Schaffert, L., Badenhorst, C. P. S., et al. (2023). Urethanases for the enzymatic hydrolysis of low molecular weight carbamates

Any alternative text (alt text) provided alongside figures in this article has been generated by Frontiers with the support of artificial intelligence and reasonable efforts have been made to ensure accuracy, including review by the authors wherever possible. If you identify any issues, please contact us.

Publisher's note

All claims expressed in this article are solely those of the authors and do not necessarily represent those of their affiliated organizations, or those of the publisher, the editors and the reviewers. Any product that may be evaluated in this article, or claim that may be made by its manufacturer, is not guaranteed or endorsed by the publisher.

Supplementary material

The Supplementary Material for this article can be found online at: https://www.frontiersin.org/articles/10.3389/fbioe.2025.1670548/full#supplementary-material

and the recycling of polyure thanes. Angew. Chem. Int. Ed. 62, e202216220. doi:10.1002/anie.202216220

Buchholz, P. C. F., Feuerriegel, G., Zhang, H., Perez-Garcia, P., Nover, L. L., Chow, J., et al. (2022). Plastics degradation by hydrolytic enzymes: the plastics-active enzymes database-PAZy. *Proteins* 90, 1443–1456. doi:10.1002/prot.26325

Cheng, H., Huang, H., Zhang, J., and Jing, D. (2017). Degradation of carbon fiber-reinforced polymer using supercritical fluids. *Fibers Polym.* 18, 795–805. doi:10.1007/s12221-017-1151-4

Chow, J., Perez-Garcia, P., Dierkes, R., and Streit, W. R. (2023). Microbial enzymes will offer limited solutions to the global plastic pollution crisis. *Microb. Biotechnol.* 16, 195–217. doi:10.1111/1751-7915.14135

Chris, B., and Nithesh Chandrasekharan, C. B. (2020). Fitting enzyme kinetics data with solver. protocols.io.

Christiansen, E., and Bakke, A. (1988). "The spruce bark beetle of eurasia," in *Dynamics of forest insect populations: patterns, causes, implications* (Springer).

Contaldo, U., Savant-Aira, D., Vergnes, A., Becam, J., Biaso, F., Ilbert, M., et al. (2024). Methionine-rich domains emerge as facilitators of copper recruitment in detoxification systems. *Proc. Natl. Acad. Sci.* 121, e2402862121. doi:10.1073/pnas. 2402862121

Da Costa, J. P., Nunes, A. R., Santos, P. S. M., Girão, A. V., Duarte, A. C., and Rocha-Santos, T. (2018). Degradation of polyethylene microplastics in seawater: insights into the environmental degradation of polymers. *J. Environ. Sci. Health, Part A* 53, 866–875. doi:10.1080/10934529.2018.1455381

Dang, H., and Lovell Charles, R. (2015). Microbial surface colonization and biofilm development in marine environments. *Microbiol. Mol. Biol. Rev.* 80, 91–138. doi:10. 1128/mmbr.00037-15

Das, M., Chacko, R., and Varughese, S. (2018). An efficient method of recycling of CFRP waste using peracetic acid. ACS Sustain. Chem. and Eng. 6, 1564–1571. doi:10. 1021/acssuschemeng.7b01456

Deng, S., Wu, J., Li, Y., Wang, G., Chai, K., Yu, A., et al. (2019). Effect of Bacillus flexus on the degradation of epoxy resin varnish coating in seawater. *Int. J. Electrochem. Sci.* 14, 315–328. doi:10.20964/2019.01.64

Dolz, M., Mateljak, I., Méndez-Sánchez, D., Sánchez-Moreno, I., Gomez De Santos, P., Viña-Gonzalez, J., et al. (2022). Colorimetric high-throughput screening assay to engineer fungal peroxygenases for the degradation of thermoset composite epoxy resins. *Front. Catal.* 2, 883263. doi:10.3389/fctls.2022.883263

Escayola, S., Bahri-Laleh, N., and Poater, A. (2024). %VBur index and steric maps: from predictive catalysis to machine learning. *Chem. Soc. Rev.* 53, 853–882. doi:10.1039/d3cs00725a

eVD (2019). Aerospace series - carbon fibre laminates - determination of the fibre, resin and void contents. 40 ed. Berlin, Germany: DIN Deutsches Institut für Normung e.V.

Feraboli, P., Kawakami, H., Wade, B., Gasco, F., Deoto, L., and Masini, A. (2011). Recyclability and reutilization of carbon fiber fabric/epoxy composites. *J. Compos. Mater.* 46, 1459–1473. doi:10.1177/0021998311420604

Geib, S. M., Filley, T. R., Hatcher, P. G., Hoover, K., Carlson, J. E., Jimenez-Gasco, M. D. M., et al. (2008). Lignin degradation in wood-feeding insects. *Proc. Natl. Acad. Sci.* 105, 12932–12937. doi:10.1073/pnas.0805257105

Gondaliya, R., Sypeck, D., and Feng, Z. (2016). "Improving damage tolerance of composite sandwich structure subjected to low velocity impact loading: experimental analysis," in 31st American Society for Composites, Williamsburg, VA, September 19-21, 2016.

Gonzalez-Garcia, R. A., Mccubbin, T., Navone, L., Stowers, C., Nielsen, L. K., and Marcellin, E. (2017). Microbial propionic acid production. *Fermentation* 3, 21. doi:10. 3390/fermentation3020021

Gräff, M., Buchholz, P. C. F., Le Roes-Hill, M., and Pleiss, J. (2020). Multicopper oxidases: modular structure, sequence space, and evolutionary relationships. *Proteins Struct. Funct. Bioinforma.* 88, 1329–1339. doi:10.1002/prot.25952

Grass, G., and Rensing, C. (2001). CueO is a multi-copper oxidase that confers copper tolerance in *Escherichia coli. Biochem. Biophysical Res. Commun.* 286, 902–908. doi:10. 1006/bbrc.2001.5474

Gu, J. D., Lu, C., Thorp, K., Crasto, A., and Mitchell, R. (1997). Fiber-reinforced polymeric composites are susceptible to microbial degradation. *J. Industrial Microbiol. Biotechnol.* 18, 364–369. doi:10.1038/sj.jim.2900401

Hilgers, R., Vincken, J.-P., Gruppen, H., and Kabel, M. A. (2018). Laccase/mediator systems: their reactivity toward phenolic lignin structures. *ACS Sustain. Chem. and Eng.* 6, 2037–2046. doi:10.1021/acssuschemeng.7b03451

Hornung, C., Poehlein, A., Haack, F. S., Schmidt, M., Dierking, K., Pohlen, A., et al. (2013). The janthinobacterium sp. HH01 genome encodes a homologue of the V. cholerae CqsA and L. pneumophila LqsA autoinducer synthases. PLOS ONE 8, e55045. doi:10.1371/journal.pone.0055045

Huang, C. C., Meng, E. C., Morris, J. H., Pettersen, E. F., and Ferrin, T. E. (2014). Enhancing UCSF chimera through web services. *Nucleic Acids Res.* 42, W478–W484. doi:10.1093/nar/gku377

Huntemann, M., Ivanova, N. N., Mavromatis, K., Tripp, H. J., Paez-Espino, D., Palaniappan, K., et al. (2015). The standard operating procedure of the DOE-JGI microbial genome annotation pipeline (MGAP v.4). *Stand. Genomic Sci.* 10, 86. doi:10. 1186/s40793-015-0077-y

Jin, F.-L., Li, X., and Park, S.-J. (2015). Synthesis and application of epoxy resins: a review. J. Industrial Eng. Chem. 29, 1–11. doi:10.1016/j.jiec.2015.03.026

Karak, N. (2021). "Overview of epoxies and their thermosets," in *Sustainable epoxy thermosets and nanocomposites* (American Chemical Society).

Khatami, S. H., Vakili, O., Movahedpour, A., Ghesmati, Z., Ghasemi, H., and Taheri-Anganeh, M. (2022). Laccase: various types and applications. *Biotechnol. Appl. Biochem.* 69, 2658–2672. doi:10.1002/bab.2313

Klose, L., Meyer-Heydecke, N., Wongwattanarat, S., Chow, J., Pérez García, P., Carré, C., et al. (2023). Towards sustainable recycling of epoxy-based polymers: approaches and challenges of epoxy biodegradation. *Polymers* 15, 2653. doi:10.3390/polym15122653

Komori, H., Sugiyama, R., Kataoka, K., Miyazaki, K., Higuchi, Y., and Sakurai, T. (2014). New insights into the catalytic active-site structure of multicopper oxidases. *Acta Crystallogr. Sect. D.* 70, 772–779. doi:10.1107/s1399004713033051

Kumar, A., and Chandra, R. (2020). Ligninolytic enzymes and its mechanisms for degradation of lignocellulosic waste in environment. *Heliyon* 6, e03170. doi:10.1016/j. heliyon.2020.e03170

Kyrpides, N. C. (1999). Genomes OnLine database (GOLD 1.0): a monitor of complete and ongoing genome projects world-wide. *Bioinformatics* 15, 773–774. doi:10.1093/bioinformatics/15.9.773

Liu, T., Shao, L., Zhao, B., Chang, Y.-C., and Zhang, J. (2022). Progress in chemical recycling of carbon fiber reinforced epoxy composites. *Macromol. Rapid Commun.* 43, 2200538. doi:10.1002/marc.202200538

Lu, S.-Y., Liu, C.-C., Huang, K.-H., Yu, C.-X., and Fu, L.-M. (2023). Microfluidic distillation system for separation of propionic acid in foods. *Micromachines* 14, 1133. doi:10.3390/mi14061133

Luukkonen, T., and Pehkonen, S. O. (2017). Peracids in water treatment: a critical review. Crit. Rev. Environ. Sci. Technol. 47, 1–39. doi:10.1080/10643389.2016.1272343

Markowitz, V. M., Chen, I. M., Palaniappan, K., Chu, K., Szeto, E., Grechkin, Y., et al. (2012). IMG: the integrated microbial genomes database and comparative analysis system. *Nucleic Acids Res.* 40, D115–D122. doi:10.1093/nar/gkr1044

Meng, F., Cui, Y., Pickering, S., and Mckechnie, J. (2020). From aviation to aviation: environmental and financial viability of closed-loop recycling of carbon fibre composite. *Compos. Part B Eng.* 200, 108362. doi:10.1016/j.compositesb.2020.108362

Mohanan, N., Montazer, Z., Sharma, P. K., and Levin, D. B. (2020). Microbial and enzymatic degradation of synthetic plastics. *Front. Microbiol.* 11, 580709. doi:10.3389/fmicb.2020.580709

Munk, L., Sitarz, A. K., Kalyani, D. C., Mikkelsen, J. D., and Meyer, A. S. (2015). Can laccases catalyze bond cleavage in lignin? *Biotechnol. Adv.* 33, 13–24. doi:10.1016/j. biotechadv.2014.12.008

Nan, Z., Xu, L., Ren, Y., Lu, J., Sun, Y., Zhang, D., et al. (2025). Recovery of carbon fibers from carbon fiber-reinforced plastics using microwave-assisted sulfuric acid treatment and reuse of recycled carbon fibers. Process. [Online] 13, 1437. doi:10. 3390/pr13051437

Naveed, M., Iqbal, F., Aziz, T., Saleem, A., Javed, T., Afzal, M., et al. (2025). Exploration of alcohol dehydrogenase EutG from Bacillus tropicus as an ecofriendly approach for the degradation of polycyclic aromatic compounds. *Sci. Rep.* 15, 3466. doi:10.1038/s41598-025-86624-5

Negi, H., Kapri, A., Zaidi, M. G. H., Satlewal, A., and Goel, R. (2009). Comparative *invitro* biodegradation studies of epoxy and its silicone blend by selected microbial consortia. *Int. Biodeterior. and Biodegrad.* 63, 553–558. doi:10.1016/j.ibiod.2009.03.001

Niemeyer, H., Schröder, T., and Watzek, G. (1983). Eine neue Lockstoff-Falle zur Bekämpfung von rinden-und holzbrütenden Borkenkäfern.

Oiffer, T., Leipold, F., Süss, P., Breite, D., Griebel, J., Khurram, M., et al. (2024). Chemo-enzymatic depolymerization of functionalized low-molecular-weight polyethylene. *Angew. Chem. Int. Ed.* 63, e202415012. doi:10.1002/anie.202415012

Padayachee, T., Nzuza, N., Chen, W., Nelson, D. R., and Syed, K. (2020). Impact of lifestyle on cytochrome P450 monooxygenase repertoire is clearly evident in the bacterial phylum firmicutes. *Sci. Rep.* 10, 13982. doi:10.1038/s41598-020-70686-8

Pardi-Comensoli, L., Tonolla, M., Colpo, A., Palczewska, Z., Revikrishnan, S., Heeb, M., et al. (2022). Microbial depolymerization of epoxy resins: a novel approach to a complex challenge. *Appl. Sci.* 12, 466. doi:10.3390/app12010466

Peng, Y., Leung, H. C., Yiu, S. M., and Chin, F. Y. (2012). IDBA-UD: a de novo assembler for single-cell and metagenomic sequencing data with highly uneven depth. *Bioinformatics* 28, 1420–1428. doi:10.1093/bioinformatics/bts174

Pinter, B., Fievez, T., Bickelhaupt, F. M., Geerlings, P., and De Proft, F. (2012). On the origin of the steric effect. *Phys. Chem. Chem. Phys.* 14, 9846–9854. doi:10.1039/c2cp41090g

Ranaei, V., Pilevar, Z., Khaneghah, A. M., and Hosseini, H. (2020). Propionic acid: method of production, current state and perspectives. *Food Technol. Biotechnol.* 58, 115–127. doi:10.17113/ftb.58.02.20.6356

Rashid, M. A., Islam, M. A., Hasan, M. N., Anu, M. N. N., and Ikbal, M. H. (2024). A critical review of dynamic bonds containing curing agents for epoxy resin: synthesis, challenges, and emerging applications. *Polym. Degrad. Stab.* 229, 110980. doi:10.1016/j. polymdegradstab.2024.110980

Scheelhaase, J., Müller, L., Ennen, D., and Grimme, W. (2022). Economic and environmental aspects of aircraft recycling. *Transp. Res. Procedia* 65, 3–12. doi:10. 1016/j.trpro.2022.11.002

Schüppel, M. S. A. D. (2023). Composites market report 2022-The global market for carbon fibers and carbon composites. Berlin, Germany: Composites United e.V.

Singh, S., Gosu, V., Upadhyaya, S., and Kumar, U. K. A. (2021). Process intensification of propionic acid separation – effect of channel geometry on microchannel distillation. *Chem. Eng. Process. - Process Intensif.* 169, 108599. doi:10.1016/j.cep.2021.108599

Studier, F. W. (2005). Protein production by auto-induction in high-density shaking cultures. *Protein Expr. Purif.* 41, 207–234. doi:10.1016/j.pep.2005.01.016

Sukanto, H., Raharjo, W. W., Ariawan, D., Triyono, J., and Kaavesina, M. (2021). Epoxy resins thermosetting for mechanical engineering. *Open Eng.* 11, 797–814. doi:10. 1515/eng-2021-0078

Tamura, K., Stecher, G., and Kumar, S. (2021). MEGA11: molecular evolutionary genetics analysis version 11. *Mol. Biol. Evol.* 38, 3022–3027. doi:10.1093/molbev/msab120

Temporiti, M. E. E., Nicola, L., Nielsen, E., and Tosi, S. (2022). Fungal enzymes involved in plastics biodegradation. *Microorganisms* 10, 1180. doi:10.3390/microorganisms10061180

The uniprot consortium (2017). UniProt: the universal protein knowledgebase. $Nucleic\ Acids\ Res.\ 45,\ D158-D169.\ doi:10.1093/nar/gkw1099$

Trinick, M. J. (1980). Relationships amongst the fast-growing rhizobia of Lablab purpureus, Leucaena leucocephala, mimosa spp., Acacia farnesiana and Sesbania grandiflora and their affinities with other rhizobial groups. *J. Appl. Bacteriol.* 49, 39–53. doi:10.1111/j.1365-2672.1980.tb01042.x

Walter, H., Hölck, O., Dobrinski, H., Stuermann, J., Braun, T., Bauer, J., et al. (2013). "Moisture induced swelling in epoxy moulding compounds," in 2013 IEEE 63rd Electronic Components and Technology Conference, Las Vegas, NV, USA, 28–31 May 2013, 1703–1708. doi:10.1109/ectc.2013.6575803

Wang, G., Chai, K., Wu, J., and Liu, F. (2016). Effect of Pseudomonas putida on the degradation of epoxy resin varnish coating in seawater. *Int. Biodeterior. and Biodegrad.* 115, 156–163. doi:10.1016/j.ibiod.2016.08.017

Wong, K.-S., Cheung, M.-K., Au, C.-H., and Kwan, H.-S. (2013). A novel Lentinula edodes laccase and its comparative enzymology suggest guaiacol-based laccase engineering for bioremediation. *PLOS ONE* 8, e66426. doi:10.1371/journal.pone.0066426

Yariv, B., Yariv, E., Kessel, A., Masrati, G., Chorin, A. B., Martz, E., et al. (2023). Using evolutionary data to make sense of macromolecules with a "face-lifted" ConSurf. *Protein Sci.* 32, e4582. doi:10.1002/pro.4582

Yoshida, S., Hiraga, K., Takehana, T., Taniguchi, I., Yamaji, H., Maeda, Y., et al. (2016). A bacterium that degrades and assimilates poly(ethylene terephthalate). *Science* 351, 1196–1199. doi:10.1126/science.aad6359

Zampolli, J., Mangiagalli, M., Vezzini, D., Lasagni, M., Ami, D., Natalello, A., et al. (2023). Oxidative degradation of polyethylene by two novel laccase-like multicopper oxidases from Rhodococcus opacus R7. *Environ. Technol. and Innovation* 32, 103273. doi:10.1016/j.eti.2023.103273

Zhang, J., Chevali, V. S., Wang, H., and Wang, C.-H. (2020). Current status of carbon fibre and carbon fibre composites recycling. *Compos. Part B Eng.* 193, 108053. doi:10. 1016/j.compositesb.2020.108053

Zhang, N., Ding, M., and Yuan, Y. (2022). Current advances in biodegradation of polyolefins. *Microorganisms* 10, 1537. doi:10.3390/microorganisms10081537

Zhang, S., Zheng, H., Chang, W., Lou, Y., and Qian, H. (2023a). Microbiological deterioration of epoxy coating on carbon steel by *Pseudomonas aeruginosa*. *Coatings* 13, 606. doi:10.3390/coatings13030606

Zhang, Y., Plesner, T. J., Ouyang, Y., Zheng, Y.-C., Bouhier, E., Berentzen, E. I., et al. (2023b). Computer-aided discovery of a novel thermophilic laccase for low-density polyethylene degradation. *J. Hazard. Mater.* 458, 131986. doi:10.1016/j.jhazmat.2023. 131986

Zotti, A., Elmahdy, A., Zuppolini, S., Borriello, A., Verleysen, P., and Zarrelli, M. (2020). Aromatic hyperbranched Polyester/RTM6 epoxy resin for EXTREME dynamic loading aeronautical applications. *Nanomaterials* 10, 188. doi:10.3390/nano10020188